Hyperfine Interact
DOI 10.1007/s10751-013-0870-1

# Effect of sintering conditions on the magnetic and structural properties of $Fe_{0.6}Mn_{0.1}Al_{0.3}$ synthesized by mechanical alloying

**J. M. Marín · Y. A. Rojas · G. A. Pérez Alcázar · B. Cruz · M. H. Medina Barreto**



**Abstract** In order to study the effect of sintering condition on the structural and magnetic behavior of prealloyed metallic powders of $Fe_{0.6}Mn_{0.1}Al_{0.3}$ system, two different thermal treatments were employed. All samples were previously milled and then compacted. Later, the sintering process was carried out in two cycles. For the first one, a sintering time of 2 h was followed by a cooling process governed by the inertia of the furnace. In the second treatment, a sintering time of 0.17 h with a controlled slow ramp of 1 °C/min between 500 °C and 250 °C. All samples were characterized by X-ray diffraction and Mössbauer spectroscopy. It was found that the sintering time improves the crystallinity while the magnetic behavior was modified by the changes in the cooling rate.

**Keywords** FeMnAl · Thermal treatment · X-ray diffraction · Mössbauer spectroscopy

Proceedings of the Thirteenth Latin American Conference on the Applications of the Mössbauer Effect, (LACAME 2012), Medellín, Colombia, 11–16 November 2012.

J. M. Marín · M. H. Medina Barreto (✉) · B. Cruz
Grupo de Investigación en Propiedades Magnéticas y Magnetoópticas de Nuevos Materiales, Departamento de Física, Universidad Tecnológica de Pereira, A. A. 097 Vereda La Julita, Pereira, Colombia
e-mail: mmedina@utp.edu.co

Y. Rojas
Grupo de Ciencia de Materiales y Tecnología del Plasma, Universidad del Tolima, A.A. 546, Ibagué, Colombia

G. A. Pérez Alcázar
Departamento de Física, Universidad del Valle, A. A. 25360, Cali, Colombia

Published online: 26 June 2013

## 1 Introduction

Fe-Mn-Al alloys have technical and scientific interest because of the presence of different properties depending on concentration and thermal treatment. It has been observed that these alloys can be prepared in several ways such as casting and mechanical alloying. In addition, if high temperature treatment takes place dramatic changes could be detected by X-ray diffraction and Mössbauer spectrometry due to ordering processes appearing at temperatures above 427 °C [1]. Mechanical alloying (MA) is a simple process based on high-energy ball milling to produce non-equilibrium powdered materials which cannot always be obtained by conventional methods, leading to nanostructured powders with different and new properties in comparison to other processes [2, 3]. Rebolledo et al. [4] show that the $Fe_{0.6}Mn_{0.1}Al_{0.3}$ system produced by MA is a soft magnetic material and this character is improved by increasing the milling time. However, the subsequent sintering leads the system to steady state with paramagnetic behavior at room temperature. Therefore, the softening during milling is lost. Furthermore, the sublimation of Mn above 527 °C affect the distribution of Mn atoms in the alloy as reported in the FeMnC system [5].

We have synthesized $Fe_{0.6}Mn_{0.1}Al_{0.3}$ steels by the complete pulvimetallurgical processes starting with prealloyed powders that were compacted and then sintered. In the process, the final structural and magnetic properties were studied using X-ray diffraction and Mössbauer spectroscopy. The milled and compacted powders were sintered up to maximum temperature of 1100 °C and then cooled in two different ways. The crystallite sizes and the mean magnetic hyperfine fields were compared against each other.

## 2 Experimental method

Using the powder metallurgy via, $Fe_{0.6}Mn_{0.1}Al_{0.3}$ powders were mechanically alloyed in a high energy planetary ball mill with a ball mass-to-powder mass ratio of 9:1 for 3, 9 and 15 h. Samples of 1,5 g were uniaxially compacted in a rigid die with a compaction force of 150 kN obtaining cylindrical pellets of 12 mm diameter and 2 mm height. Green samples were sintered in a tubular furnace by using a heating rate of 10 °C/min until was reached a maximum temperature of 1100 °C in argon atmosphere to prevent oxidation. The cooling of the test tubes was performed using two different cycles. Cycle I (Fig. 1a) has a sintering time of 2 h and then cooled at the rate of the inertia of the oven (cooling of the resistance). In the Cycle II (Fig. 1b) the same sintering temperature was considered, but the sintering time was 0.17 h. In this case, the cooling was performed using the furnace inertia rate until 500 °C and then with a programmed ramp until 250 °C, lowering the temperature at a rate of 1 °C/min. X-ray patterns were taken at room temperature in a Bruker D8 Advance difractometer. Mössbauer spectra were collected using a $^{57}$Fe source in standard transmission geometry. Data from the difractograms was refined with the Rietveld method by GSAS (General Structure Analysis System) software [6], and Mössbauer spectra were fitted with MOSFIT program.

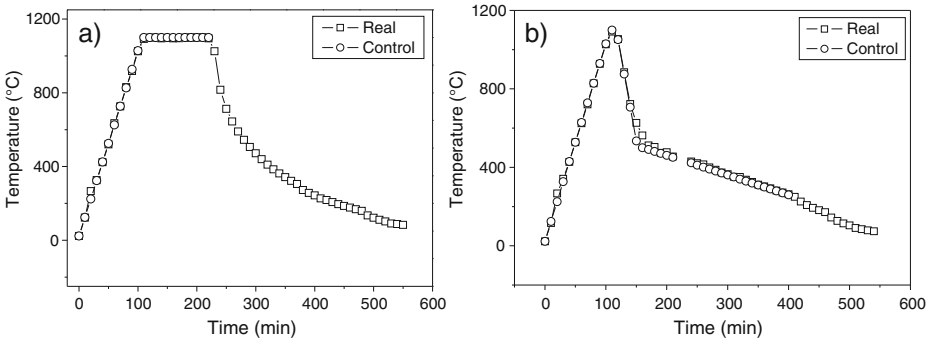


**Fig. 1** Sintering cycles (**a**) Cycle I and (**b**) Cycle II

## 3 Results and discussion

Figure 2 shows some of the X-ray patterns acquired from powders milled (3 and 9 h), compacted and sintered for both cycles. All the studied samples exhibit the presence of a bcc structural phase, showing characteristic diffraction peaks of the planes (110), (200) and (211). The presence of the bcc phase suggests that the Mn and Al atoms are distributed inside the Fe cell. For short milling times, the alloy is not completely consolidated, but after sintering a full diffusivity of the minor elements is achieved and the reached lattice parameter is around 0,2902 nm (±0,0001 nm), in agreement with previous results obtained by milling [4, 7]. This value is independent of the sintering method employed, slightly above the typical lattice parameter of pure iron (0,2870 nm). This enhancement of the lattice parameter is due to the presence of Al which presents a bigger atomic size compared to that of the Fe atom, and is in according with previous results reported for melted and ordered Fe-Al alloys [8, 9] as well as grinded and heat treated Fe-Al alloys [10–12].

The crystallite size in the $Fe_{0.6}Mn_{0.1}Al_{0.3}$ consolidated samples was obtained from the refinement made by GSAS. Figure 3 shows that the crystallite size values increase for the sintered samples in the Cycle I, in comparison to the values in Cycle II. Therefore, an improvement in the crystallinity is found. A similar behavior has been reported in magnetic materials [13, 14] as well as in non-magnetic materials [15].

Results acquired from Transmission Mössbauer Spectroscopy (TMS) at room temperature for 3, 9 and 15 h in the Cycle I, are shown in Fig. 4a. The spectra display the formation of a magnetically disordered phase and a broad paramagnetic line near the central region. The fitting realized with the MOSFIT program exhibits the presence of two components: a broad singlet and a hyperfine field distribution (HFD) between 60 kOe and 300 kOe. Figure 4b shows the probability function for the hyperfine field distribution. This type of fit, and remembering the XRD results which show only the presence of a bcc Fe-Mn-Al lattice, indicates that this lattice is disordered and composed by different ferromagnetic Fe sites, which explain the HFD, and paramagnetic Fe sites, which explain the paramagnetic line. The ferromagnetic Fe sites are those rich in Fe and the paramagnetic ones are those rich in Al, as it has been found in previous reports of these type of samples [4, 16].

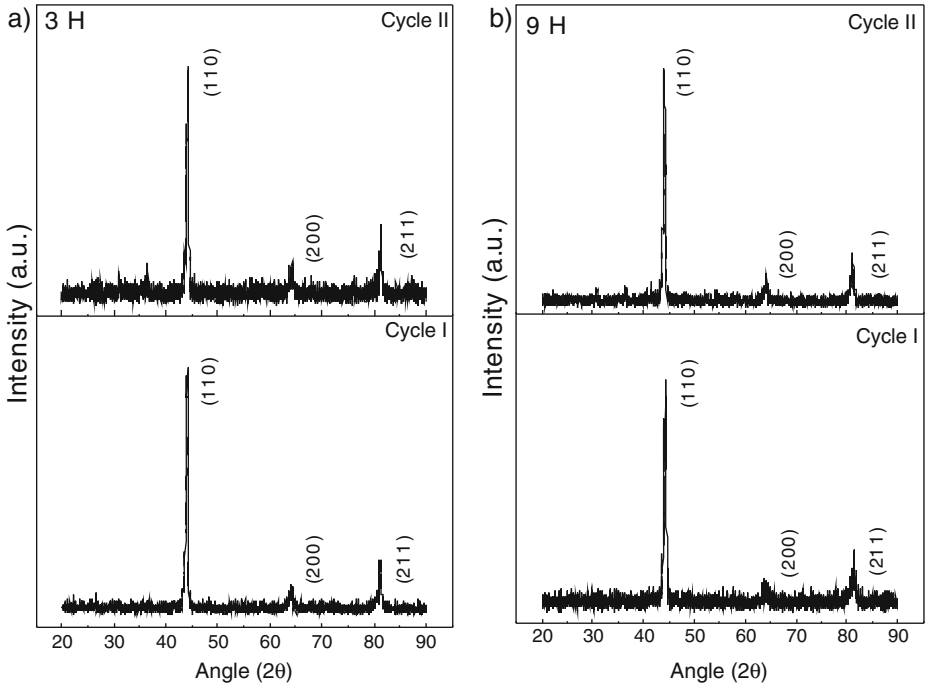


**Fig. 2** X-Ray difractograms from both cycles for 3 and 9 h of milling

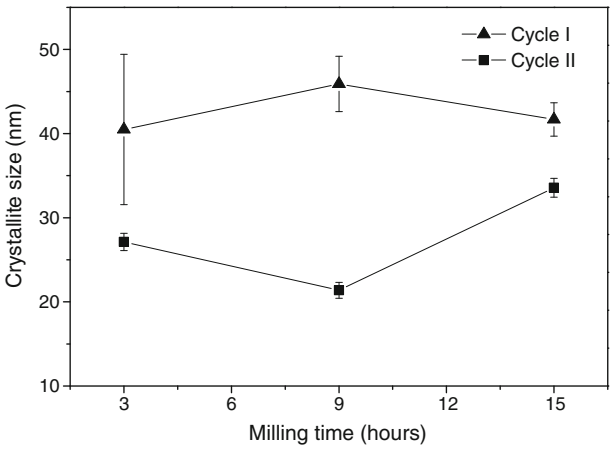


**Fig. 3** Crystallite size evolution over milling time and sintering cycle

Figure 5a shows the Mössbauer spectra and their corresponding HFDs of the $Fe_{0.6}Mn_{0.1}Al_{0.3}$ samples sintered by using Cycle II. The fitting process was similar to those obtained with the cycle I, with the presence of a singlet and a hyperfine field distribution between 30 kOe and 300 kOe. Figure 5b shows the respective probability function for the hyperfine field distribution. However, the relative percentual amount of each component shows variations for each cycle, as can be observed

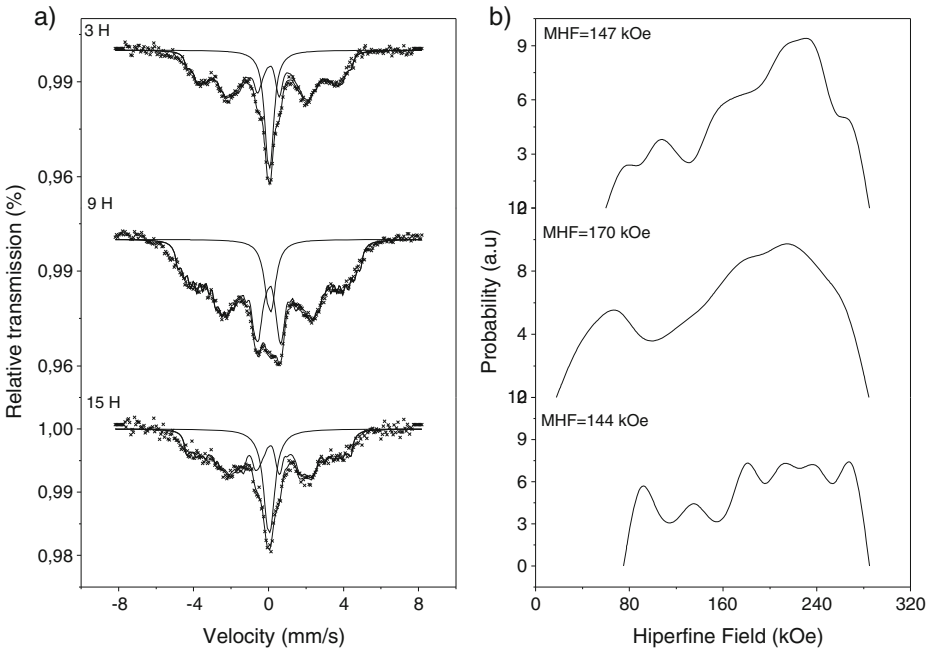


**Fig. 4** Room temperature Mössbauer spectra (**a**) fitted by MOSFIT for Cycle I against milling time and (**b**) probability function for the hyperfine field distribution

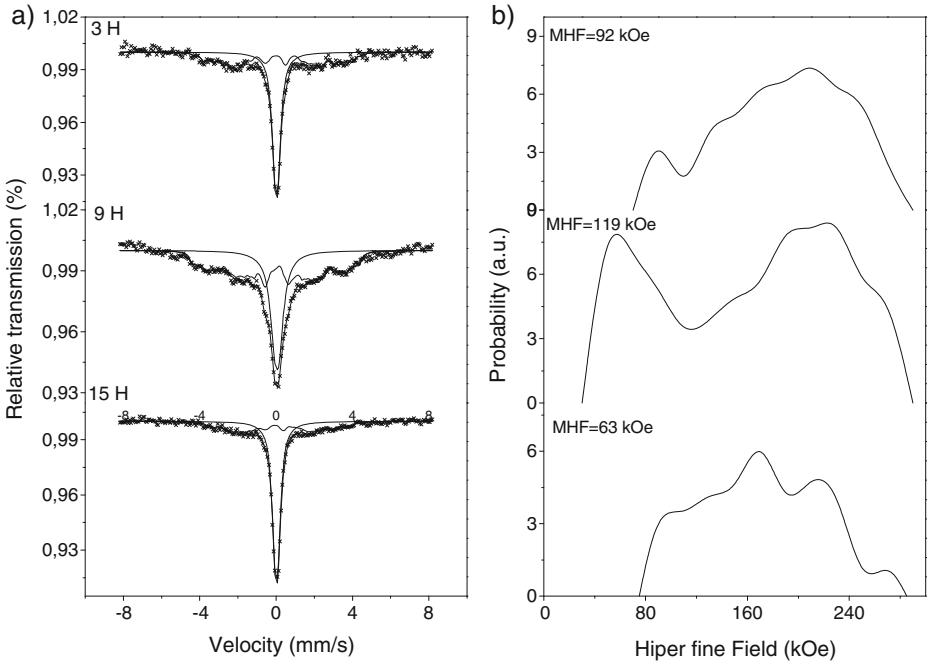


**Fig. 5** Room temperature Mössbauer spectra (**a**) fitted by MOSFIT for Cycle II against milling time and (**b**) probability function for the hyperfine field distribution

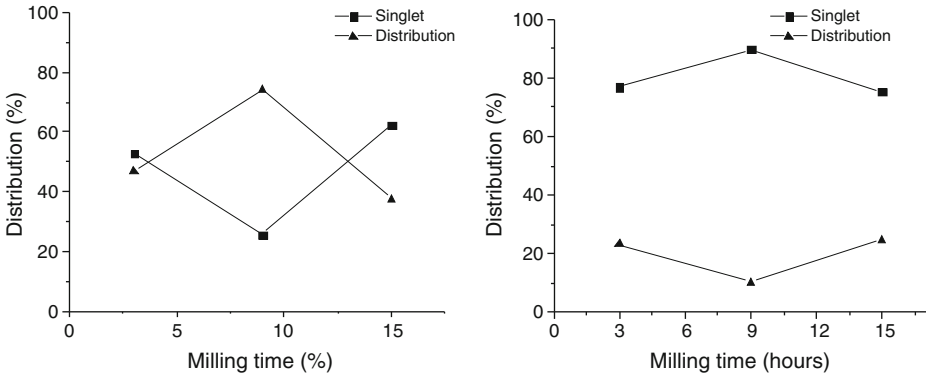


**Fig. 6** Distribution percentages for both sintering cycles: Cycle I (*left*) and Cycle II (*right*)

**Fig. 7** Mean hyperfine field variation against milling time and sintering cycle

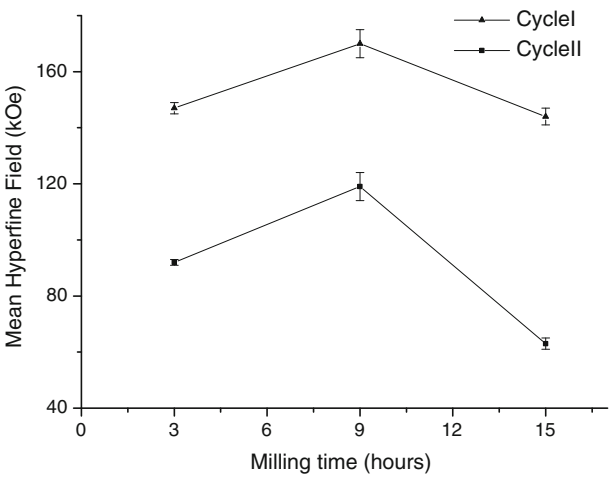


in Fig. 6. For Cycle II there is a greater presence of the singlet (about 80 %). Conversely, there is not a clear predominant component in Cycle I. This behavior may be related to configurational changes that occur in the neighborhood of the iron atoms. A sintering time of 2 h combined with a faster cooling (≈2,4 °C/min between 500 °C and 250 °C) in Cycle I allowed to retain part of the magnetic disorder which was present at high temperature. With the slower cooling of Cycle II (≈1 °C/min between 500 °C and 250 °C) and also shorter sintering time, the magnetic accommodation of the atoms inside the alloy reveals a steady state more stable (in our case, a paramagnetic one) and a decrease of the disorder degree. These results are in agreement with reports in $Fe_{60}Al_{40}$ alloys where these systems are paramagnetic when they are ordered and ferromagnetic when they are disordered [17, 18]. Regarding the relationship of the cooling rate with variations on magnetic properties, Thota et al. [19] have found that changes in the neighborhood of an iron atom and the quantity of the relative phases presents a clear dependance respecting cooling conditions.

Finally, Fig. 7 shows the mean hyperfine field for the samples treated with both cycles. The sintered systems obtained in the Cycle I has a higher mean hyperfine fields then that in the Cycle II. This behavior can be properly related to variations in the crystallite size derived from the diffractograms refinement; thereby, crystallite sizes of the order of 40 nm to 45 nm generate a mean hyperfine field near to 160 kOe, while crystallite sizes between 20 nm and 30 nm show approximate 38 % decrease in the mean hyperfine field, independent from milling time. Thus, variations in the mean hyperfine field exhibit an increase in the long-range order of the crystals benefited from rapid cooling, favoring the ferromagnetic interactions of Fe atoms with its neighborhood.

## 4 Conclusions

In conclusion, according to the established parameters during the thermal treatment, changes on the structural and magnetic properties $Fe_{0.6}Mn_{0.1}Al_{0.3}$ disordered alloy obtained via powder metallurgy were achieved. Independently of the thermal treatment employed, samples exhibited a bcc structure and the coexistence of two phases: a paramagnetic component and a disordered ferromagnetic component. Nevertheless, in the diffraction patterns a relation between crystallite size and sintering time was revealed. Additionally, an increment on the long-range order of the crystals reached by a faster cooling and a longer sintering time, favors the presence of a disordered magnetic phase.

**Acknowledgements** Authors would like to thank Universidad Tecnológica de Pereira for its financial support under project **3-12-3**. J.M. Marín is grateful with Colciencias for the scholarship in the "Jóvenes Investigadores e Innovadores" program.

## References

1. Bremers, H., Frick, M., Hesse, J.: Hyperfine Interact. **94**(1), 1855–1859 (1994)
2. Suryanarayana, C.: Prog. Mater. Sci. **46**, 97–103 (2001)
3. Song, H., Wu, Y., Tangm, C., Yuan, S., Gong, Q., Liang, J.: Tsinghua Sci. Technol. **14**(3), 300–306 (2009)
4. Rebolledo, A., Romero, J., Cuadrado, R., GonzÍez, J., Pigazo, F., Palomares, F., Medina, M.H.: J. Magn. Magn. Mater. **316**, 418–421(2007)
5. Hryha, E., Dudrova, E., Tadashi, M. (eds.): ISBN: 978-953-307-980-6, InTech, Available from: http://www.intechopen.com/books/application-of-thermodynamics-to-biological-and-materials-science/the-sintering-behaviour-of-fe-mn-c-powder-system-correlation-between-thermodynamics-and-sintering-pr (2011)
6. Larson, A., Dreele, R.V.: General structure analysis system (GSAS). Los Alamos National Laboratory Report LAUR, pp. 86–748 (2000)
7. Pérez Alcázar, G.: Rev. Acad. Colomb. Cienc. **28**(107), 265–274 (2004)
8. Taylor, A., Jones, R.M.: J. Phys. Chem. Solids **6**, 16 (1958)
9. Pérez Alcázar, G.A., Galvão da Silva, E.: J. Phys. F, Met. Phys. **17**, 2323 (1987)
10. Apianiz, E., Plazaola, F., Garitaonandia, J.S., Martin, D., Jiménez, J.A.: J. Appl. Phys. **93**(10), 7649–7651 (2003)
11. Martin Rodríguez, D., Apianiz, E., Plazaola, F., Garataoandia, J.S., Jiménez, J.A., Schmool, D.S., Cuello, G.J.: Phys. Rev. B **71**, 212408 (2005)
12. Nogués, J., Apianiz, E., Sort, J., Amboage, M., d'Astuto, M., Mathon, O., Puzniak, R., Fita, I., Garitaonadia, J.S., Suriñac, S., Muñoz, J.S., Baró, M.D., Plazaola, F., Baudelet, F.: Phys. Rev. B **74**, 024407 (2006)

13. Singh, J.P., Payal, R.S., Srivastava, R.C., Agrawal, H.M., Chand, P., Tripathi, A., Tripathi, R.P.: J. Phys. Conf. Ser. **217**, 1–4 (2010)
14. Abdoli, H., Asgharzadeh, H., Salahi, E.: J. Alloy. Compd. **473**, 116–122 (2009)
15. Garcia, S., Portelles, J., Martinez, F., Font, R., Quiñones, J.R., Siqueiros, J.M.: Rev. Mex. Fís. **49**(1), 15–19 (2003)
16. Valderruten, J., Pérez, G., Civale, L.: J. Mater. Sci. **39**, 5445–5449 (2004)
17. Das, G.P., Rao, B.K., Jena, P., Deevi, S.C.: Phys. Rev. B **66**, 184203 (2002)
18. Gialanella, S., Amils, X., Baró, M.D., Delcroix, P., Le Caer, G., Lutterotti, L., Suriñach, S.: Acta Mater. **46**, 3305 (1998)
19. Thota, H., Garg, A., Pandey, B., Verma, H.C.: Hyperfine Interact. **187**, 1–184 (2001)